TRENDS IN THEORETICAL PHYSICS

Volume I

Based on the 1988–89 Distinguished-Speaker Colloquium Series of the Theoretical Physics Institute at the University of Minnesota.

EDITED BY

P.J. Ellis
and
Y.C. Tang

Addison-Wesley Publishing Company
The Advanced Book Program
Redwood City, California • Menlo Park, California • Reading, Massachusetts
New York • Don Mills, Ontario • Wokingham, United Kingdom • Amsterdam
Bonn • Sydney • Singapore • Tokyo • Madrid • San Juan

Publisher: *Allan M. Wylde*
Production Manager: *Jan V. Benes*
Electronic Production Consultant: *Lori Pickert*
Promotions Manager: *Laura Likely*
Cover Design: *Iva Frank*

Library of Congress Cataloging-in-Publication Data

Trends in theoretical physics / [edited by] Paul J. Ellis. Y. C. Tang.
p. cm.
Papers presented at a colloquium series started in the fall of 1988 at the School of Physics and Astronomy of the University of Minnesota.
Includes bibliographical references (p.).
1. Mathematical physics. 2. Astrophysics. 3. Nuclear physics.
I. Ellis, Paul J. II Tang, Y. C.
QC20.T69 1990 530.1—dc20 90-28373
ISBN 0-201-50393-X

ABCDEFGHIJ-MA-89

3

Detecting the Quark-Gluon Plasma

G. Bertsch
Dept. of Physics and Cyclotron Lab.
Michigan State University
East Lansing, MI 48824

3.1 Introduction

What are the properties of matter at high temperature and density? This question is the focus of a large program of research in high energy heavy ion physics. Besides general interest, there are two particular reasons for this study. First, the theory of Quantum Chromodynamics (QCD), which is the accepted theory of strong interaction physics, is capable in principle of predicting these properties. Lattice calculations suggest that a phase transition may take place at a temperature of about 200 MeV.

Another reason for interest in matter at high temperature is that the universe in the Big Bang is thought to have originated at high density and cooled through these temperatures. If there were a first order phase transition, it could have important consequences for the later evolution. For example, baryonic matter might become more concentrated as a result of the phase transition; this would affect the later nucleosynthesis into elements.

To study hot matter, we first need a way to produce it. The only possibility in the laboratory is to collide heavy nuclei at high energy. Obviously high energy is needed, but why use nuclei instead of nucleons or other hadrons? It is important that the hot matter reaches a local equilibrium

under the conditions of study. Only then does the concept of temperature have meaning. If we were condensed matter physicists, and we doubted the equilibrium, we could just leave the sample in the oven longer. That isn't possible here; the high temperature lasts only a short time. The conditions for equilibration become more favorable by making the region of the high energy density as large as possible. And that is done using heavy nuclei as projectiles rather than hadrons.

There are two accelerators involved in this program. In Brookhaven, the AGS has accelerated heavy nuclei up to 15 GeV/n in experiments starting from 1987. This program is now in full operation, and interesting results are presently emerging. In Geneva at CERN the large accelerator SPS accelerates ions up to 200 GeV/n, in an experimental program that started in 1986. Both CERN and Brookhaven use ions of lighter mass elements, mainly oxygen and sulfur. The CERN program had a major running period in 1987, and the main results that I discuss come from this run. These results were presented in a conference in 1987, and have since been published [1].

As I will try to explain, the results are interesting and consistent with the expected phase transition, but proof is still lacking. Future experiments starting in 1990 should do better; I have particular expectations for measurements of pion correlations. Further experiments are under discussion at CERN using beams of accelerated lead nuclei. This would allow substantially higher energy density to be reached. Finally, there are plans in the USA to build a heavy ion collider at Brookhaven, to collide 200 GeV/n nuclei against each other. This might take the system out of the mixed state of hadronic matter and plasma, into a state of superheated plasma.

My own interest in this subject started from the point of view of nonrelativistic heavy ion physics. There we deal with a system that is extremely complicated to describe in detail. Nevertheless one is able to calculate with fair confidence certain kinds of observables, particularly those involving conserved quantities such as linear momentum. Classical simulations of the collision turn out to be very useful providing the quantum effects of the Pauli principle are included. So it is natural to try analogous simulations of the ultrarelativistic collisions. There are two important differences between these regimes, however. In lower energy heavy ion collisions, we believe we understand the important degrees of freedom and how they interact. One can then make a complete dynamical calculation, starting from the cold nuclei approaching the collision region. In the ultrarelativistic domain, we do not know in enough detail how the important degrees of freedom, the partons in the nucleons, interact to make reliable calculations. On the other hand, the dynamics in the low energy domain is not so favorable for determining the equation of state. The equilibration process takes a considerable fraction of the total collision time, so that the observables are sensitive to

the details of the equilibration as well as to the equation of state. It has so far not been possible to extract equation of state information from these experiments. The equilibration should be more favorable in the ultrarelativistic domain. Simple estimates based on expected densities of partons indicate that the system would quickly come to local equilibrium. It is thus reasonable to pursue models in which the details of the formation of the hot matter are ignored, and instead assume a local equilibrium at a certain time. This is my attitude and all inferences are based on this assumption. But we must keep in mind that it is essentially untested as of yet.

3.2 Initial Conditions

Before we can model the dynamics of the expanding hot matter, we need to know how the system starts out. The appearance of the hot zone for a 200 GeV/n Oxygen nucleus colliding with a Gold target nucleus is shown pictorially in Fig. 3.1. We view the collision in the midrapidity frame, so both nuclei are Lorentz contracted. The left figure shows the mass distributions at the point when the surfaces just touch. The right figure shows the nuclei and the hot zone between them at the time 1 fm/c later. The excitation is in a roughly cylindrical zone; it expands longitudinally at the projectile velocity, i.e. close to the velocity of light. The transverse motion is less clear and depends on the details of the dynamics that we wish to study.

For our initial conditions, we assume some distribution of energy in this cylindrical interaction zone. Experiments already tell us quite a bit about that energy distribution. Essentially, we only have to look at the projected mass overlap between the projectile and the target to determine the transverse distribution of energy. This is the conclusion of the experiments that measure the so-called transverse energy produced in the collision. The transverse energy E_T is defined as the sum over final state particles

$$E_T = \sum_i E_i \, sin\theta_i \ , \tag{3.1}$$

where E_i and θ_i are the energies and angles of the emerging particles. The probability distribution of this quantity follows quite closely the behavior expected if the energy is produced according to the geometric overlap of the projectile and target nucleons. This is illustrated in Fig. 3.2. On the horizontal axis is the transverse energy, and the differential cross section in this variable is plotted. The two graphs show data from Brookhaven [2] and from CERN [3]. A peak in the distribution is seen at small transverse energy. This is due to peripheral collisions. At higher transverse energy the

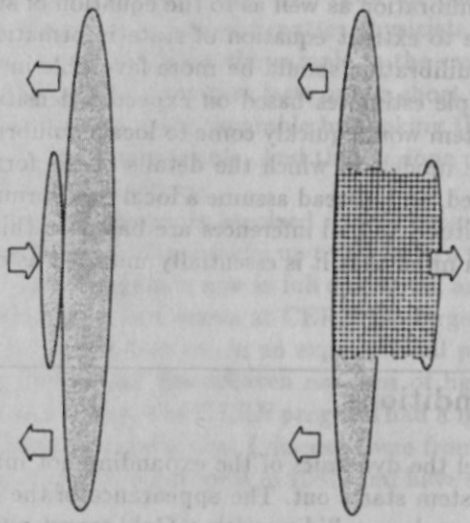

FIGURE 3.1
Visualization of a central collision between oxygen and gold nuclei. The oxygen beam has an energy of 200 GeV/n, i.e. a rapidity of $y = \cosh^{-1}(200/0.931) = 6.06$, but the system is viewed in the midrapidity frame, $y = 3.03$. Thus both target and projectile are Lorentz-contracted by a factor $\gamma = \cosh 3.03 = 10.4$. The right drawing shows the positions of the nuclei 1.5 fm/c after they first make contact.

cross section has a plateau, corresponding to more central impact parameters. Finally, the distribution falls exponentially above a certain point.

The shape of the transverse energy distribution is very easy to understand geometrically. One calculates the number of collisions between nucleons, assuming that the nucleons are distributed in (Lorentz-contracted) spheres having the volume of the nucleus, and they move only in the longitudinal direction. In Fig. 3.2a, each nucleon-nucleon collision is assumed to produce a certain distribution of transverse energy. These contributions are then convoluted with the distribution of NN collisions. The theoretical distribution for the Brookhaven experiment is shown in the figure, with the contributions from different numbers of NN collisions separately graphed. The overall curve agrees very well with experiment.

I still have to explain how the distribution of transverse energy for individual NN collisions is determined. In the analysis of Fig. 3.2a it was parameterized to fit the data. A more fundamental analysis, modelling the

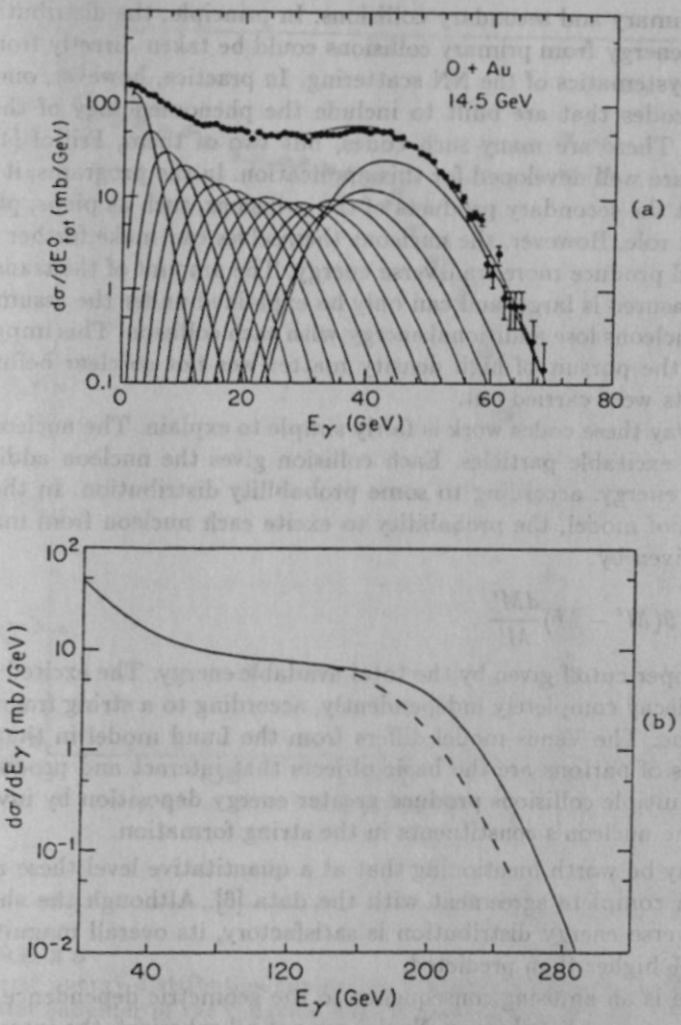

FIGURE 3.2
Transverse energy distribution. a) is from 14.5 GeV/n collisions of O + Au, measured at Brookhaven. The experimental data is fit by a sum of functions representing convoluted NN transverse energy distributions. b) is from 200 GeV/n collisions of O + Au, measured at CERN (dashed line). The solid line is the prediction of the VENUS code, which assumes independent parton collisions in the target and projectile nucleons.

underlying NN dynamics, has been applied to interpret the higher energy data from CERN. To calculate from the NN collisions, we need to distinguish primary and secondary collisions. In principle, the distribution of transverse energy from primary collisions could be taken directly from the empirical systematics of the NN scattering. In practice, however, one uses computer codes that are built to include the phenomenology of the NN scattering. There are many such codes, but two of them, Fritiof [4] and Venus [5], are well developed for this application. In the programs, it is assumed that the secondary products of the collisions, such as pions, play no subsequent role. However, the nucleons themselves can make further interactions and produce more transverse energy. The amount of the transverse energy measured is large, and can only be explained under the assumption that the nucleons lose additional energy with each collision. This important finding in the pursuit of high density matter was not so clear before the experiments were carried out.

The way these codes work is fairly simple to explain. The nucleons are treated as excitable particles. Each collision gives the nucleon additional excitation energy, according to some probability distribution. In the case of the Fritiof model, the probability to excite each nucleon from mass M to M' is given by

$$dP \sim \theta(M' - M)\frac{dM'}{M'}\,, \tag{3.2}$$

with an upper cutoff given by the total available energy. The excited nucleons then decay completely independently, according to a string fragmentation scheme. The Venus model differs from the Lund model in that pairs and triples of partons are the basic objects that interact and produce the strings. Multiple collisions produce greater energy deposition by involving more of the nucleon's constituents in the string formation.

It may be worth mentioning that at a quantitative level these models are not in complete agreement with the data [6]. Although the shape of the transverse energy distribution is satisfactory, its overall magnitude is about 20% higher than predicted.

There is an amusing consequence to the geometric dependence of the transverse energy distribution. Nuclei are not all spherical; the intercepted mass of a deformed nucleus will depend on its orientation. The maximum mass is presented when the projectile goes along the major axis of a deformed target. Conversely, when the target is oriented with the major axis transverse to the beam, the overlap will be smaller. Thus the shoulder on the distribution of the transverse energy should be less sharp in the case of deformed nuclei. This can be seen in Fig. 3.3, taken from data by the Helios collaboration [7]. The two targets compared are tungsten (W) and platinum (Pt). These differ in mass by only about 10 units out of nearly

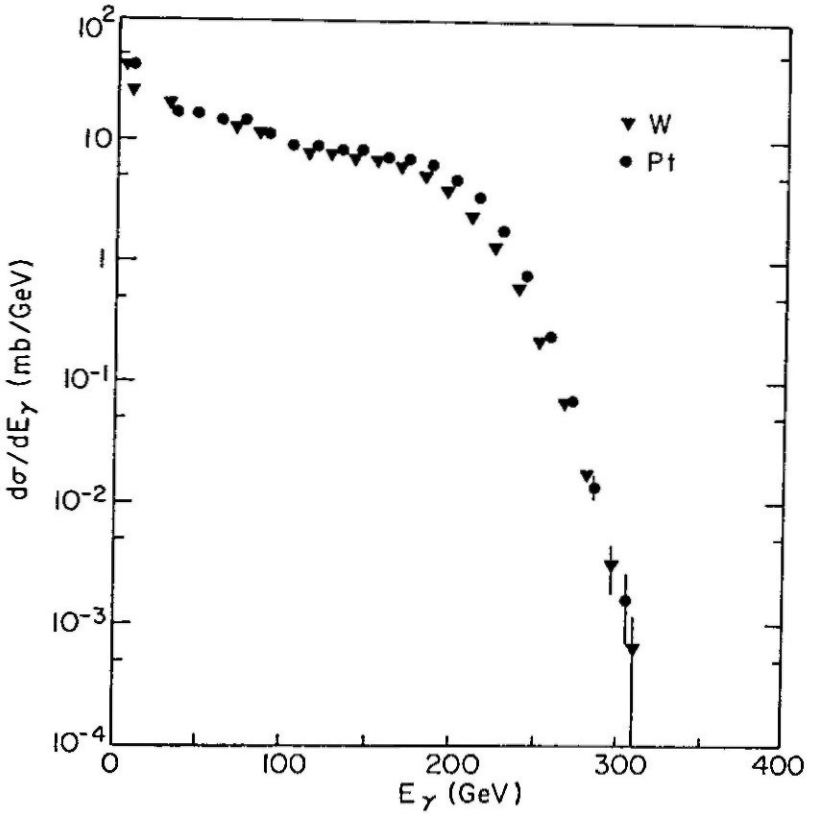

FIGURE 3.3
Transverse energy distribution comparing tungsten and platinum targets. The softer shoulder of the tungsten data is explained by nuclear deformation effects.

200, but W is deformed while Pt is spherical. It may be seen that the shoulder is broader in the case of W, as expected.

Having established how the energy is distributed spatially in the direction transverse to the beam, we next ask about the longitudinal distribution of energy. There are two extreme models which have been explored. One of these, proposed by Bjorken [8], is quite simple from an analytic point

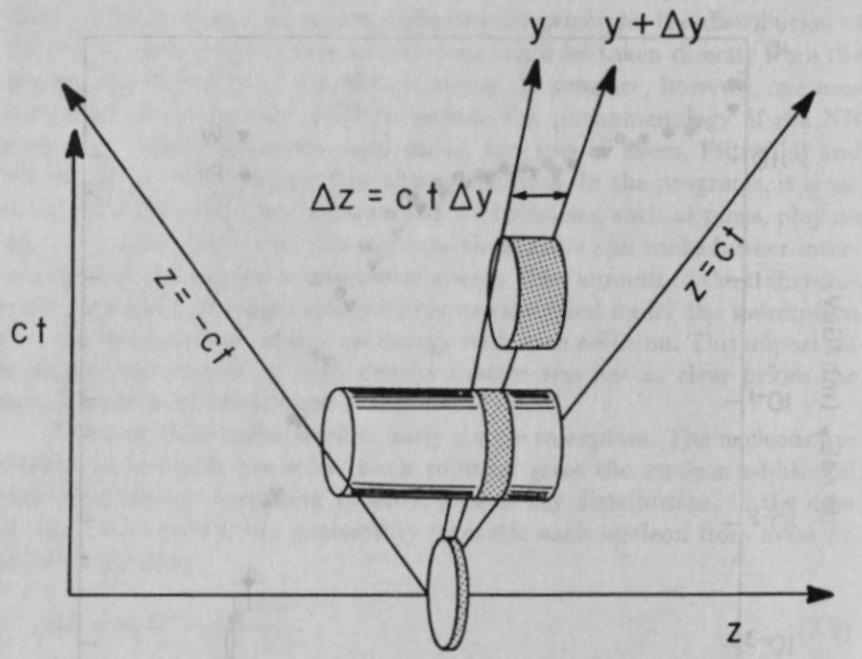

FIGURE 3.4
Time development of the hot matter in Bjorken's boost invariant expansion.

of view. The longitudinal distribution of energy is assumed to be boost-invariant. That is, the hot zone in Fig. 3.1 should look the same in other frames besides the one we chose. For nearby frames, we see the target and projectile discs receding from the collision point at a velocity close to c. The hot matter is locally at rest at the collision point, i.e. it has no net longitudinal motion at the collision point. Thus, the average rapidity of the matter does not change in a comoving frame. This is illustrated in Fig. 3.4. Consider a small slice of the cylinder, bounded by planes moving with rapidities y and $y + \Delta y$. From the Lorentz kinematics, $z = \tau \sinh y$ and $t = \tau \cosh y$, we find that the volume in the slice varies with time as $\Delta V = \Delta z A = c\tau \Delta y A$, where A is the cross sectional area of the cylinder. In the Bjorken model, the flux of entropy across any transverse surface is zero and there is no transport of entropy from one region of rapidity to another. Thus, in the absence of entropy-producing processes, a measurement

of entropy in the final state can be extrapolated back to the collision time. Specifically, if dS/dy is the entropy per unit rapidity in the final state, and σ is the entropy density, then the relation is

$$dS/dy = \sigma A c t \ . \tag{3.3}$$

In Bjorken's model the final state observables should be independent of rapidity. This is very nearly the case for the average transverse momentum of the final state particles. However, the number of particles per unit rapidity is not constant over a broad range. The rapidity distribution is better described empirically by a Gaussian,

$$dn/dy \approx exp(-\frac{(y-y_0)^2}{2y^{*2}}) \ . \tag{3.4}$$

The variance of the Gaussian is about $y^* = 1.5$ for the CERN experiments. This kind of behavior is predicted by Landau's hydrodynamic model [9]. In the Landau model one assumes that the collision brings the matter to rest in some intermediate rapidity frame, and the spatial distribution of matter is a disc, due to the Lorentz contraction. The highest gradient of the density is along the beam axis, so the matter is accelerated most along that direction. The resulting rapidity distribution resembles a Gaussian.

Of these two extreme models, the Bjorken model is probably more realistic. According to the more microscopic pictures such as contained in the Fritiof model, the energy deposition is via string fragmentation. If the strings were of infinite extent, they would break in a boost-invariant way. The lack of boost invariance in the final state reflects the finite size effects of the ends of the strings and the initial distribution of strings in rapidity.

In the calculations that I will describe below, my collaborators and I used the Bjorken assumption. I don't believe that the results would be much different if a more realistic longitudinal distribution of energy were assumed. The main effect would be that the system would evolve from a higher entropy density, since matter would be accelerated out of the midrapidity region.

3.3 Equation of State

I have mentioned entropy without explaining how it is measured. In fact we cannot measure it in the thermodynamic sense, because there is no adiabatic energy transfer. If the system is in local thermal equilibrium, the entropy density can be calculated from the temperature. For a gas of massless particles, the relation from statistical mechanics is [10]

$$\sigma = \frac{4\pi^2}{90}(n_B + \frac{7}{8}n_F)T^3 \ , \tag{3.5}$$

where n_B and n_F are the number of species of bosons and fermions, respectively. We pretend that the final state is a gas of massless pions, with $n_\pi = 3$, so the formula for the entropy density in the hadronic phase is

$$\sigma_\pi = \frac{2\pi^2}{15} T^3 \,. \tag{3.6}$$

The formula for the number density of particles has the same T-dependence,

$$\rho_\pi = n_\pi \int \frac{d^3p}{8\pi^3} \frac{1}{exp(p/T) - 1} = \frac{3\zeta(3)}{\pi^2} T^3 \tag{3.7}$$

The entropy per particle is then given by the ratio of Eq. (3.6) to Eq. (3.7), $S_\pi = \sigma_\pi / \rho_\pi \approx 3.6$. So the way we estimate the entropy of the final state is to count the number of pions and multiply by 3.6.

We now need some dynamics to evolve the initial state that was constructed. Our goal is to measure the equation of state, but the best we can do is to try out various models and compare with experiment. The motivation for modelling in general was explained by Weisskopf in the following anecdote:

> "A model is like an Austrian railroad timetable. Austrian trains are always late. A foreign visitor asked the conductor on an Austrian train, why they even bother printing the timetables. The conductor's reply: How else would we know how late the trains are?"

In our model of the equation of state the low density phase is assumed to be an ideal gas of massless pions. Then the entropy function is given above in Eq. (3.6), and the pressure is

$$P_\pi = \sigma_\pi T/4 \,. \tag{3.8}$$

The quark-gluon phase is also treated as a gas of massless particles. The entropy density is determined from Eq. (3.5). To count the number of species of particle, note that each kind of quark is described by a Dirac equation, having 4 degrees of freedom. We consider two flavors of quark, "u" and "d", and three colors. Thus $n_F = 4 \cdot 2 \cdot 3 = 24$. The gluons have two helicities and 8 colors, making $n_B = 16$. The coefficient in parentheses in the entropy formula is thus $16 + 24 \cdot 7/8 = 37$, which is more than an order of magnitude higher than in the lower density phase. Thus at the transition temperature the two phases will have very different entropy densities. This is also the case for the energy densities in the two phases.

The only difference from the massless particle thermodynamics in the model of the quark-gluon phase is in the pressure and energy formulas. The pressure consists of two terms, the first of which is the pressure due to the particle motion. This has the same form as Eq. (3.5). The second term is

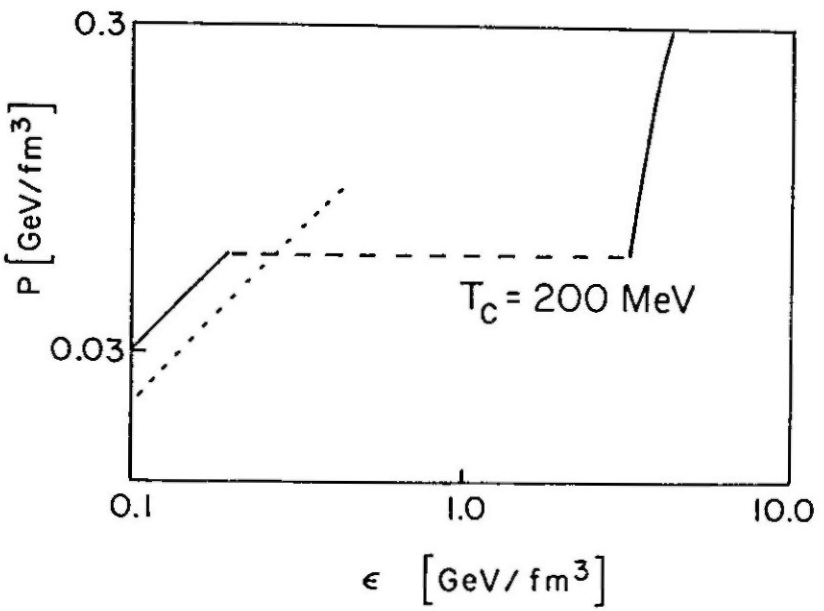

FIGURE 3.5
The equation of state in the simple pion gas/quark-gluon bag model, as a function of energy density. The short-dashed line shows the hadronic equation of state when all light-quark mesons are included.

a constant, the so-called "bag" pressure. The total is

$$P_{qg} = \frac{\sigma_{qg} T}{4} - B \,. \tag{3.9}$$

At the transition temperature the two pressures are equal, which gives a condition relating it to B. We consider the transition temperature (or B) as a parameter of the model, to be determined if possible by the data. A graph of the equation of state is shown in Fig. 3.5, plotting pressure as a function of energy density [11]. On the left is the pure pion gas phase, on the right the pure plasma phase, and the flat region in the middle is the mixed phase. Note that the mixed phase extends over an order of magnitude in density, for the reason given above. In the figure is also shown the equation of state of a hadronic gas consisting of the light-quark mesons: π, ρ, ω, and η. The

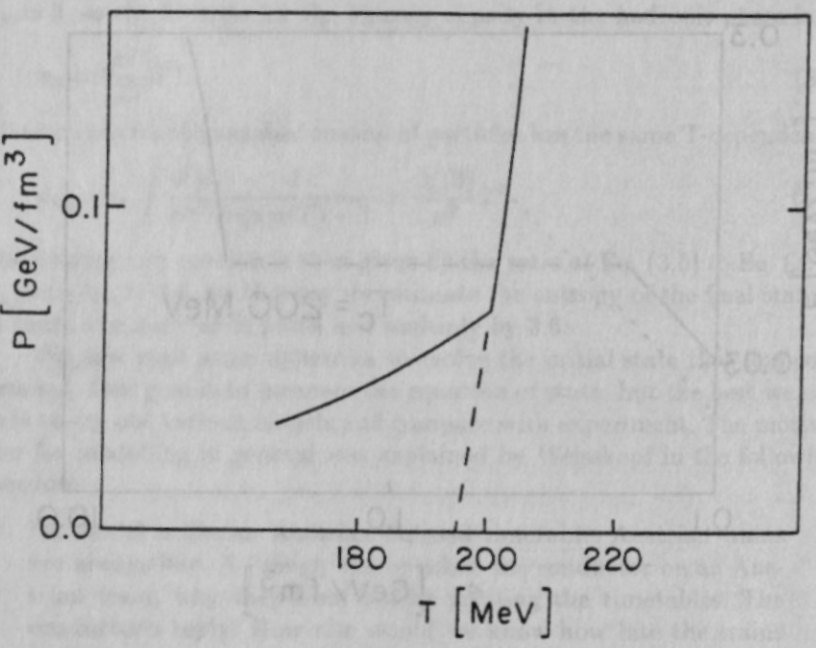

FIGURE 3.6
Equation of state in the simple model, as a function of temperature. The dashed line shows a possible metastable region of the quark-gluon phase.

more particles that are included, the lower will be the pressure for a given energy density. In fact, it was suggested a long time ago that there might be so many particles that any amount of energy could be put into the system at a certain limiting temperature. The pressure would then also approach a limiting value. The only way to distinguish these models qualitatively is to go the quark-gluon phase, where QCD predicts a renewed increase in pressure.

In Fig. 3.6 the equation of state is shown with temperature as the independent variable. Note that the pressure changes much more rapidly with temperature in the plasma phase than in the pion phase. We can imagine cooling the system from the plasma phase, creating a metastable plasma state of lower pressure. If the phase transition is first order, some metastability is expected.

The lattice gauge calculations of QCD are not yet settled enough to

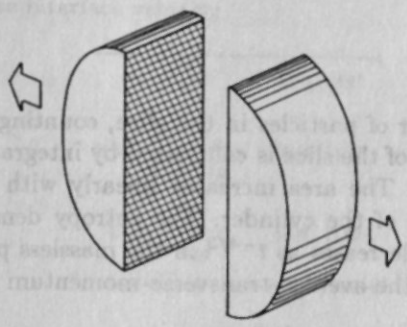

FIGURE 3.7
Geometry for the argument relating pressure to transverse momentum in Eqs. (3.10) and (3.11).

replace simple models of high density such as I described above. The magnitude of the entropy jump from one phase to the other is consistent with the simple model, at least in some calculations [12]. In calculations with only gluon fields, the transition appears to be first order, although the full entropy density of the plasma phase may not be present immediately above the transition temperature. Technical difficulties associated with quarks on the lattice prevent any definite statements about the phase transition when both quark and gluon degrees of freedom are included.

3.4 Observables

Assuming now that we have an equation of state and can calculate the dynamics of the expanding hot matter, what should we measure? I believe two observables are particularly relevant to the study of the equation of state. One quantity is the average transverse momentum of the particles in the final state. As emphasized by Van Hove [13], the transverse momentum directly reflects the pressure history of the expansion. We can see this in a semiquantitative way by examining a slice through the cylinder of hot expanding matter. We cut the slice in half, as in Fig. 3.7, and ask how much force is exerted on the cut. This force transfers momentum between the two halves, and thus produces transverse momentum in the final state particles. Suppose the two halves have momentum p_{slice} and $-p_{slice}$ and

that the average motion respects the axial symmetry of the cylinder.. Then the average transverse momentum of the particles contained in the slice is given by

$$< p_t >= \frac{2p_{slice}}{\pi N} , \tag{3.10}$$

where N is the number of particles in the slice, counting both sides. The transverse momentum of the slice is calculated by integrating the pressure P over area and time. The area increases linearly with time due to the longitudinal expansion of the cylinder. The entropy density decreases as t^{-1}, and the pressure decreases as $t^{-4/3}$ in the massless pion model of the hadronic phase. Then the average transverse momentum is given by

$$< p_t >= \frac{2}{\pi N} \int PdAdt \sim t^{2/3}|_{\tau_0}^{\tau_f} . \tag{3.11}$$

The dependence on the equation of state is obvious in this relation. A stiff equation of state has more pressure at a given entropy density and produces a higher average transverse momentum. Conversely, if a phase transition makes the equation of state very soft, there would not be more transverse momentum produced, despite a higher energy density.

However, note that the integral in Eq. (3.11) is not very well behaved. It diverges at the upper limit. The integral must be cut off at the freezeout time τ_f, when interactions cease. The dependence on the initial time is less important, but still could be significant. For these reasons, much more detailed calculations are required to interpret the experiments.

The time duration and spatial extent of the strongly interacting stage of the collision are also important characteristics which might indicate a possible phase transition. The space-time distribution of the interacting zone can be measured by pion correlations, as will be explained later. The time measurement is particularly interesting. In the bag model of the phase transition, the matter must be rarified by more than an order of magnitude to convert it completely to the other phase. If there is an interface separating the two phases, this severely limits the rate at which the phase transition can take place. The interface travels into the plasma, converting dense plasma into pion gas. However, the flux of entropy in the pion gas is bounded by c times its entropy density. Thus the interface cannot move faster than c times the ratio of entropy densities. This slow phase conversion produces a long-lived plasma droplet. In Table 3.1, I quote some of the estimates of this phase conversion that may be found in the literature. Assuming that the phase conversion rate is c/10, a droplet of initial radius 2 fm would last 20 fm/c. This is a very long time compared to duration times based on collision rates in an expanding pion gas.

TABLE 3.1
Estimates of phase interface velocity

$v \leq \frac{1}{6}c$	Ref. [14]
$v = \frac{2}{3\sqrt{3}}\frac{\epsilon_\pi}{\epsilon_{qg}}c$	Ref. [15]
$v = \frac{1}{4}\frac{\epsilon_\pi}{\epsilon_{qg}}c$	Ref. [16]

3.5 Detailed Models

I now turn to the specific analytic and numerical models for dealing with the expansion dynamics. The simplest model is Bjorken's, which assumes pure longitudinal expansion. As mentioned before, the boost invariance and the assumption of entropy conservation imply that the entropy per unit rapidity is constant and the entropy density decreases as t^{-1}. Since all other quantities can be expressed in terms of the entropy density as the independent variable, the entire evolution of the system is fixed. The model exhibits a long-lived mixed state because of the limited expansion rate from purely longitudinal motion. Clearly the neglect of transverse expansion is a drastic approximation, requiring better modeling. We saw in Eq. (3.11) that the freezeout time is an important parameter of the evolution; in the Bjorken model the system never freezes out [17]. To remedy this deficiency it is necessary to calculate the transverse expansion explicitly. The evolution can then no longer be determined analytically; the price one pays for the more accurate modelling is that the results are strictly numerical. Hydrodynamic calculations have been reported in Refs. [18,19]. In these calculations, one still must assume something about the freezeout, typically that it occurs at a certain density or a certain temperature. Also, the phase transition dynamics in hydrodynamics is rather complicated, with the possibility of rarifaction shocks and entropy production. The hydrodynamic conservation laws are insufficient to specify the details of the transition under these conditions.

For these reasons a more detailed model was made by McLerran together with myself and others [16]. To avoid the uncertainties of freezeout, we decided to simulate the evolution of the pionic final state. By tracking coordinates of the individual pions, we could see how they collide and determine the spatial and temporal size of the collision region as well as

the transverse momentum distribution. This model needs pi-pi scattering cross sections as input. Even though nobody has measured the scattering process, we were able to extract adequate information about the scattering from the literature.

We simulated the dense phase of matter by a collection of droplets of appropriate density. The droplets are assumed to have the same initial size, and this is taken as a parameter of the model. However, the range of this parameter is somewhat limited. A droplet radius smaller than about 1 fm would make the concept of a separate phase doubtful, since the QCD size scale is of the order of 1 fm. Very large droplets, say 2 fm radius or larger, would produce obvious fluctuations in the rapidity distribution of the final state particles.

The conversion of matter from one phase to the other is treated by a model very similar to the compound nucleus model of neutron evaporation from a nucleus [20]. The hadronic state is produced by emission of pions from the droplet surface. The rate of emission is determined by detailed balance, assuming that the droplet absorbs all incident pions. The resulting formula for the emission rate W is

$$W = \frac{c}{4}\pi R^2 \rho_\pi(T)\,, \tag{3.12}$$

where $\rho_\pi(T)$ is the density of pions at temperature T, given by Eq. (3.7). Our model neglects the interaction between the droplets; because the droplets are quite heavy their thermal motion is small.

With these ingredients we can simulate the evolution of the system from the start of the phase transition to the final state. The time at which the phase conversion begins of course varies for different longitudinal rapidities due to time dilation. We fill the cylinder with randomly placed droplets, which begin emitting pions at the proper time corresponding to the beginning of the phase transition. The evolution of the system proceeds by time steps; in each step pions may be emitted or absorbed from droplets, they may scatter from each other, and they of course change position due to their velocity. After a long enough time, all interactions cease and the properties of the final state pions are saved in a file. The information about the pions that we need to save is their momenta and the coordinates of their last interaction point. That could be be where they last collided with another pion, or where they were emitted from a droplet.

In general, our results from the cascade modelling confirm the previous hydrodynamic calculations. In hydrodynamics, the dense phase stays within the original zone of creation. The droplets in our model also tend to remain close to their point of origin, because they are so massive. Very little entropy production was found in the hydrodynamic phase transition, and the droplets also do not produce much entropy when they evaporate pions.

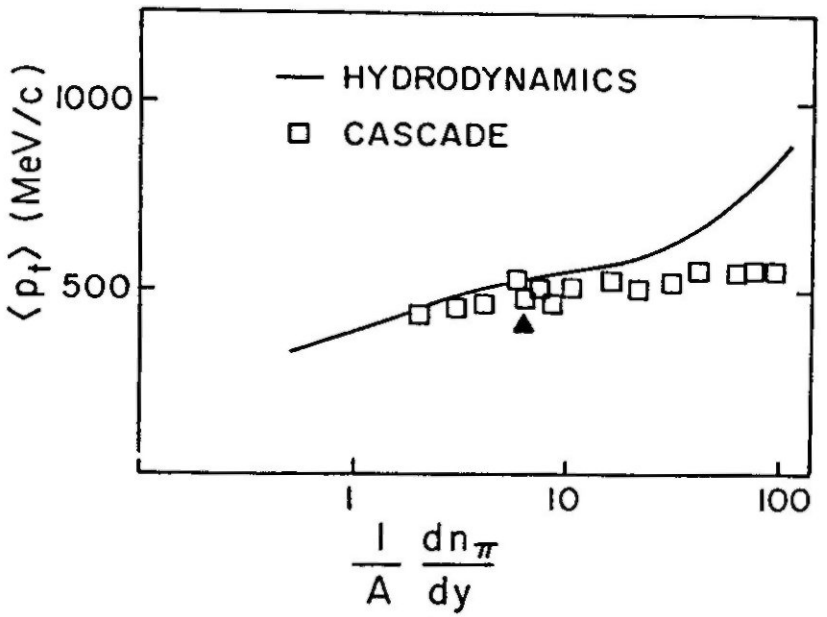

FIGURE 3.8
Final state transverse momentum as a function of the rapidity density of the produced pions. The solid line is the hydrodynamic prediction of Ref. [19], and the squares are the results of the cascade calculation of Ref. [16]. The experimentally measured point from O + Au collisions at CERN is shown by the triangle.

It can be shown that an isolated droplet radiating pions would produce 30% more pions than one converting to the pion phase under adiabatic conditions. This difference is not very much, when we compare with the order of magnitude difference in entropy densities expected for the two phases.

One more qualitative conclusion is worth mentioning. We found relatively little interaction between the pions in the hadronic state. On the average, each pion makes about one collision on the way out. These collisions do not affect the momentum distribution of the pions very much, so the final state pions almost provide a direct view of the plasma droplet surface.

Turning to the quantitative results, the model predicts the average

transverse momentum, which can be displayed as a function of the rapidity density of particles in the final state. The graph, shown in Fig. 3.8, is the closest we can come with experimentally measurable quantities to the equation of state graph in Fig. 3.5. The cascade model, shown with squares, is compared with the hydrodynamic model, shown as the solid line. In the hydrodynamic model, a trace of the phase transition physics is seen in the slope of the curve. At low particle densities, the system is always in the pion gas phase. The flattening of the curve at intermediate densities is due to the mixed phase. Finally, at the highest densities the system starts in a plasma phase and the transverse momentum rises more rapidly.

The cascade model was applied assuming the same phase transition temperature (200 MeV) as in the hydrodynamic model, and the two models agree very well for the pion phase and the mixed phase regimes. We did not put the internal pressure of the plasma droplets into the cascade model, so the increased momentum in the superheated phase is not reproduced. In any case, the agreement of these two different numerical approaches is encouraging that the numerics of relating the equation of state to observable quantities is under control.

3.6 Experiment

Let us now take a closer look at the experimental data. I divide the experiments into two categories. In one class are the experiments that measure qualitative effects, such as the suppression or enhancement of flavored meson production. This kind of experiment is valuable to show the degree of interaction and equilibration in the hot zone. However, measurement of the equation of state requires experiments that determine dimensional quantities such as momentum. The relevant data here can be summarized in a few sentences. I take as a typical collision ^{16}O on a heavy target, with a projectile momentum of 200 MeV/n. The density of pions in the final state goes to about 120 per unit of rapidity. The data used to obtain this number is shown in Fig. 3.9. Only π^- were measured, so the number from this graph is multiplied by 3 to get the total pion yield. As mentioned earlier, to get so many pions in the final state requires that both primary and secondary collisions deposit energy into the central region. We see on the graph that the central region extends from about 1.5 to 3.5 units of rapidity, where the pion density has a broad peak.

The average transverse momentum of these pions is 400 MeV/c, which is only 10% higher than in NN collisions. Experimentalists were probably disappointed when they found such a small difference between heavy ion

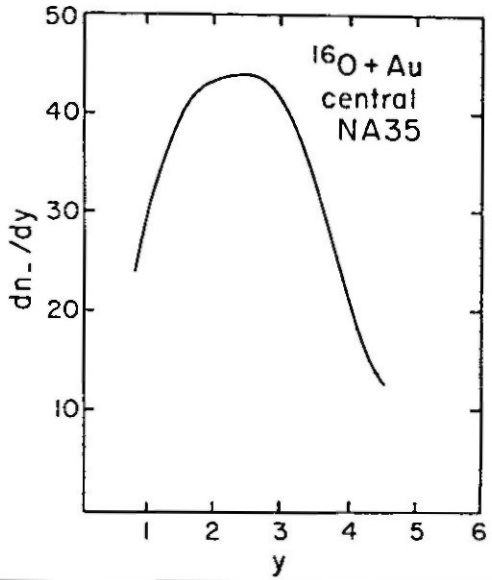

FIGURE 3.9
Experimental pion rapidity distribution for central O + Au collisions at 200 GeV/n, from Ref.[1], p. 92.

and NN collisions. But this is exactly what to expect if the system goes into a mixed phase. I have put the data point from these measurements on Fig. 3.8, the experimentalist's equation-of-state graph. The transverse momentum is in fact slightly lower than predicted for a phase transition at T=200 MeV.

At this point I should mention a feature of the pion momentum spectrum that is not explained so far and is very puzzling. The transverse momentum distribution of the pions, shown in Fig. 3.10, has an excess of low momentum pions that are not present in NN collisions. Comparing NN and heavy ion distributions, one finds that about 1/4 of the final state pions are in this low momentum group. A suggestion has been made that the effect may be due to a cooling of the pions by radial expansion [21], but this idea is not supported by the cascade or hydrodynamic calculations. Another possibility is that the pions are somehow associated with slow-moving baryons; again no detailed estimates supporting this idea have been published. Obviously, it is necessary to understand this data before any firm conclusions can be made that are based on the assumption of local equilibrium.

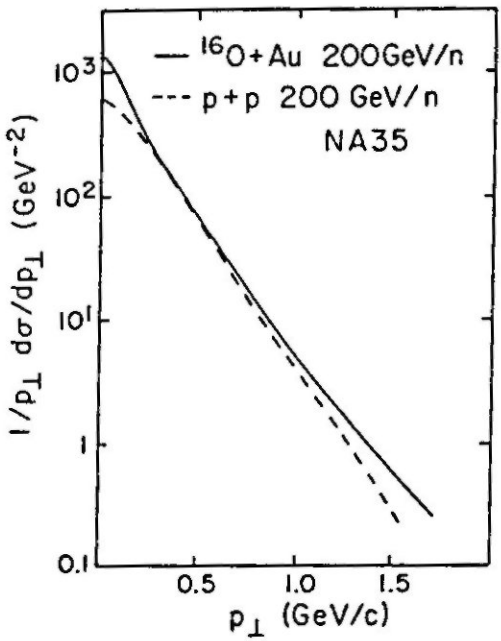

FIGURE 3.10
Momentum spectrum of the pions from central O + Au collisions at 200 GeV/n, from Ref. [1], p. 96.

3.7 Pion Interferometry

I now want to discuss a completely different kind of measurement, called pion interferometry or HBT interferometry [22]. Identically charged pions have correlations due to their Bose statistics, and these correlations reflect the distribution in space and time of the source of the pions. The theory of this effect may be shown in a few steps starting from the wave function for a pair of pions,

$$\begin{aligned}\psi_{\pi\pi} &= \frac{1}{\sqrt{2}}\left(e^{ip_1\cdot r_1+ip_2\cdot r_2}+e^{ip_1\cdot r_2+ip_2\cdot r_1}\right)\\ &= \sqrt{2}e^{\frac{1}{2}iK\cdot(r_1+r_2)}cos(\frac{1}{2}q\cdot(r_1-r_2))\,,\end{aligned} \tag{3.13}$$

where $q = p_1 - p_2$ is the difference in momentum between the pions and $K = p_1 + p_2$ is their sum. The amplitude to create the pions is given by

the overlap with some source function $s(r)$,

$$A \approx \int dr_1 dr_2 s_1(r_1) s_2(r_2) \psi_{\pi\pi} \ . \tag{3.14}$$

The modulus squared of this overlap is the probability to produce the pions with the given momenta. It simplifies under the assumption of an incoherent source, by which is meant

$$< s_i(r_1) s_i(r_2) > \approx G(r_1)\delta(r_1 - r_2) \ . \tag{3.15}$$

Then the probability integral becomes

$$P(q) \approx 1 + \int dr_1 dr_2 G(r_1) G(r_2) cos(q \cdot (r_1 - r_2)) \ . \tag{3.16}$$

Thus the measurement of $P(q)$ gives direct information about the Fourier transform of the source function $G(r)$. In making this argument, we assumed that the pions are created at the same time. Eq. (3.16) is applicable to the more general case of different creation times if $q \cdot r$ is interpreted as the 4-vector dot product. It is useful to use the equal time wave function, however, because interactions such as the Coulomb interaction can be included by replacing the free wave function by the appropriate scattering wave function in a potential.

In this analysis, the assumption of an incoherent source restricts one to large spatial sources. The quality of the data tends also to be limited, so that one can only extract one or two parameters describing the source size. In any case, the results of this analysis are very different for hadronic sources and for the heavy ion collisions. For a hadronic source the correlation tends to be independent of the direction of the correlation; the source size is small, about 1 fm [23]. The correlations between pions in the CERN heavy ion collisions show a much larger source size, of the order of 6 fm [24].

The expectations for the source parameters are very different, depending on whether or not there are long-lived heavy particles produced as intermediates. The source for the two extreme scenarios, hot pion gas or plasma droplet initial state, are depicted in Fig. 3.11. We imagine observing a slice of the cylinder in a frame in which the pions come out with zero longitudinal motion. The two transverse directions to the axis of the cylinder we denote as outward and sideward. The outward direction is along the direction of motion of the pions, and the sideward is perpendicular to the pion direction and the cylinder axis. If the pions are formed immediately in a hot gas, their density is very hot and they make many collisions before the freezeout. These collisions take place as the gas expands, and the source is much larger radially than the initial cylinder. However, as pointed out by Pratt [25], these pions will be moving radially outward so that the pions on

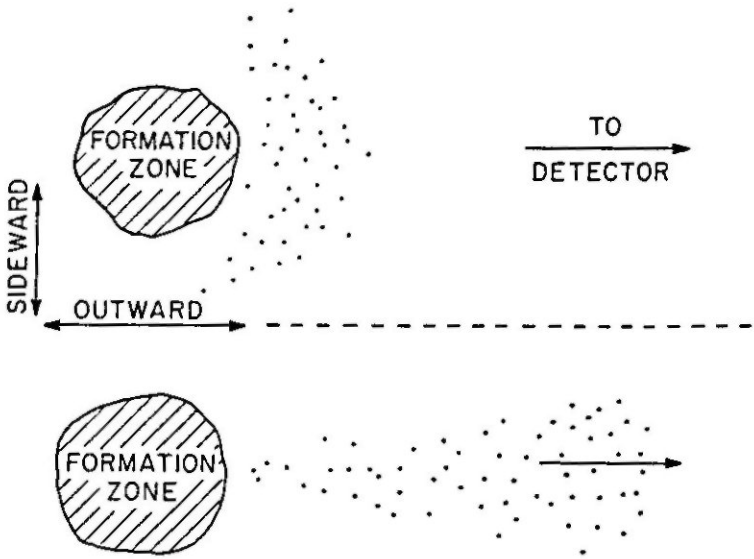

FIGURE 3.11
Pion source distribution in transverse direction, for two scenarios of the evolution. The upper diagram depicts the source points for a hot pion gas, showing only pions that are moving in the direction of the detector. The lower diagram depicts the corresponding pions from a decaying plasma phase. The horizontal elongation is due to the time delay converting high density matter to the low density phase.

the opposite side of the cylinder will not go into the detector. Effectively, the source seen by the detector just covers a region in front of the formation zone. This is depicted in the figure. In the plasma droplet scenario, the pions evaporate rather slowly so the spatial source size in the outward direction becomes long, as depicted in the figure. So the characteristic of heavy droplet formation is a long outward source and a moderately small sidewards source.

To test this idea quantitatively, I generated a pion source function $G(r)$ from the cascade simulation. But first an important technical point: the pions' momenta as well as their positions is determined by the source function, so we must explicitly include a dependence on p as well as r in G. We took the source function to be [26]

$$G(r,p) = \sum_i \delta^4(r - r_i) exp(-\frac{(p-p_i)^2}{p_0^2}) , \tag{3.17}$$

where the sum runs over the final state pions produced by the cascade simulation. The p_0 is a smoothing parameter. The expression we evaluate to get the correlation is then the same as Pratt's formula [25]

$$P(q,K) = 1 + \frac{\int d^4r d^4r' G(r,K/2)G(r',K/2)cos(q\cdot(r-r'))}{\int d^4r d^4r' G(r,p_1)G(r',p_2)} . \tag{3.18}$$

It is conventional to parameterize the source function by a Gaussian, in which case the correlation is also Gaussian. If we write the source function as

$$G(r,p) = exp(-(\frac{r_l}{R_l})^2 - (\frac{r_{side}}{R_{side}})^2 - (\frac{r_{out}}{R_{out}})^2) exp(-(\frac{p}{p_0})^2) , \tag{3.19}$$

then the correlation function is simply

$$P = 1 + exp(-\frac{1}{2}((q_l R_l)^2 + (q_{side}R_{side})^2 + (q_{out}R_{out})^2) . \tag{3.20}$$

The sideward and outward dimensions resulting from the cascade simulation are shown in Fig. 3.12. In the lower corner on the left side are the correlation lengths obtained for the hot pion gas model, *i.e.* all the pions were assumed to be already formed at the initial time (taken as $\tau_0 = 1$ fm/c). One of the points shows the correlations if the pions freely traveled from this point without interaction. The source size then reflects only the transverse size of the projectile nucleus, which is 2.2 fm in the case of ^{16}O. The nearby point on the graph shows the results with pion scattering included. The physical source size is much larger, but hardly any effect is seen in the correlation, for the reason explained above.

A dramatically different correlation function is obtained in the plasma droplet scenario. The outward dimension becomes much larger. For droplets of radius 1 fm, the outward dimension is about 10 fm/c. This increases for droplets with larger initial radii; smaller initial radii do not have much effect. The large source radius found experimentally [24] could arise from the droplets. To confirm this, it is necessary to separate the outward and sideward dimensions, which unfortunately is not so easy with the present experimental data. However, there are indications that the large dimension is associated with the outward direction [27]. One possible problem connected with this interpretation should be mentioned [28]. More massive mesons than the pion are formed in the collision, and their decay lifetimes will contribute to a larger source size. In particular, the ω meson with a mean life of 20 fm/c produces decay pions that masquerade as a long-lived source. The effect is substantial when meson production rates of the Lund model are used in the calculation. However, the Lund model predicts a

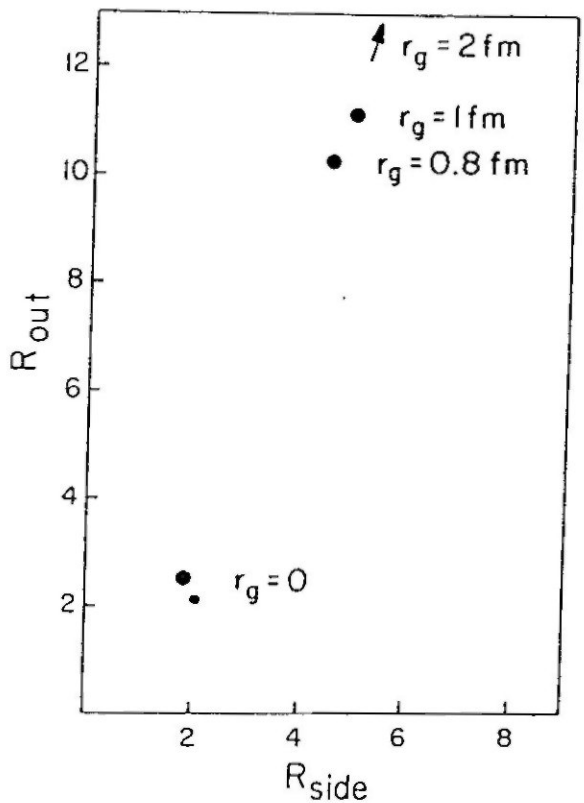

FIGURE 3.12
Comparison of outward and sideward source sizes from the cascade simulation. The formation zone is a boost-invariant cylinder with a Gaussian radius parameter 1.8 fm, producing hot matter that evolves to a final state containing 120 pions per unit rapidity. The small point near the origin shows the dimensions if the pions are formed immediately and do not interact. Collisions between points in the hot pion gas hardly change the source size, as shown by the nearby larger point. Models with plasma droplet formation give very large outward dimensions. For initial droplet radius 0.8 fm and 1.0 fm, the outward dimension is about 10 fm/c. Increasing the droplet radius to 2.0 fm doubles the outward dimension.

rather high proportion of ω mesons in the final state. If the collisions allow local thermal equilibrium, the proportion would be much lower. It is also found that in NN collisions the proportion of ρ mesons, while substantial, is less than assumed in the Lund model.

3.8 Outlook

Clearly, the data looks promising, suggesting that high density matter has been created and that it disperses with moderate pressure on a moderately long time scale. However, we need to know more about the equilibration. On the experimental side, one can imagine more sophisticated experiments that would measure proportions of higher mesons such as the ρ and the η. The strange mesons are interesting also, although we do not expect as rapid an equilibration in strangeness as in the degrees of freedom associated with ordinary quarks.

It is also important for theorists to estimate the time scales for equilibration using more fundamental descriptions of the hadronization process. One study reported an equilibration time of 2.5 fm/c, using a parton model of the nucleons [29]. On the other hand, hadronization times are much shorter in the Lund model [30]. On a fundamental level, the QCD parton structure of a nucleus may differ in important respects from a collection of independent nucleons. Collisions between the partons with the modified probability distribution may take place on rather short time scales, of the order of 0.3 fm/c [31,32]. Clearly, this is an area where more work needs to be done.

Acknowledgements

The author acknowledges conversations with L. McLerran, L. Van Hove, and W. Willis. This work was supported by the National Science Foundation under Grant PHY 87-14432.

Bibliography

[1] Z. Physik **C38** (1988), published as a separate book by Springer Verlag.

[2] *ibid*, p. 39.

[3] T. Akesson *et al.*, Phys. Lett., to be pub. This is the Helios collaboration.

[4] B. Andersson, G. Gustafson, and B. Nilsson-Almqvist, Nucl. Phys. **B281** (1987) 289.

[5] K. Werner, Phys. Lett. **B208** (1988) 520.

[6] T. Awes, priv. comm.

[7] T. Akesson *et al.*, Phys. Lett., to be pub.

[8] J.D. Bjorken, Phys. Rev. **D27** (1983) 140.

[9] L.D. Landau, *Collected Works*, p. 569-585; Izv. Akad. Nauk Ser. Fiz. 17 (1953) 51.

[10] For the statistical mechanics of massless bosons, see any text on blackbody radiation, *e.g.*, L. Landau and E. Lifshitz, *Statistical Physics* (Addison Wesley, Reading, MA, 1958) p. 165.

[11] The energy densities of the two phases are given by: $e_{pi} = 3\sigma_{pi}/4$ and $e_{qg} = 3\sigma_{qg}/4 + B$.

[12] T. Celik *et al.*, Nucl. Phys. **B256** (1985) 670.

[13] L. Van Hove, Phys. Lett. **B118** (1982) 138.

[14] L. Van Hove, Z. Physik **C27** (1986) 135.

[15] P. Danielewicz and P.V. Ruuskanen, Phys. Rev. **D35** (1987) 344.

[16] G. Bertsch, M. Gong, L. McLerran, V. Ruuskanen and E. Sarkkinen, Phys. Rev. **D37** (1988) 1202.

[17] An exercise for the student: show that the one-dimensional hydrodynamics never freezes out by finding the total number of collisions a particle makes. This is estimated as $\int dt < \sigma v \rho >$ where σ is a cross section, $v \approx c$ is a relative velocity. The particle density, ρ, has a time dependence given by the considerations in the text.

[18] G. Baym, B. Friman, J. Blaizot, M. Soyeur, and W. Czyz, Nucl. Phys. **A407** (1983) 541.

[19] H. von Gersdorff, L. McLerran, M. Kataja, and P. Ruuskanen, Phys. Rev. **D34** (1986) 794; M. Kataja, P. Ruuskanen, L. McLerran, and H. von Gersdorff, Phys. Rev. **D34** (1986) 2755.

[20] V. Weisskopf, Phys. Rev. **52** (1937) 295.

[21] T.W. Atwater, P.S. Freier and J. Kapusta, Phys. Lett. **199** (1987) 30; K. Lee and U. Heinz, Regensburg preprint, 1988.

[22] The initials HBT stand for the authors of the paper where the technique of using boson correlations to infer a source size was first proposed, R. Hanbury-Brown and R. Twiss, Nature **177** (1956) 27. The technique was introduced to hadronic physics using pion correlations by G. Goldhaber, S. Goldhaber, W. Lee and A. Pais, Phys. Rev. **120** (1960) 300.

[23] T. Akesson,*et al.*, Z. Phys. **C36** (1987) 517.

[24] A. Bamberger *et NA35 al.*, Phys. Lett. **B203** (1988) 320.

[25] S. Pratt, Phys. Rev. Lett. **53** (1984) 1219.

[26] G. Bertsch, M. Gong, and M. Tohyama, Phys. Rev. **C37** (1988) 1896.

[27] J. Harris, *Proc. Quark Matter '88* (Lenox, MA), Nucl. Phys., to be pub.

[28] M. Gyulassy and S. Padula, *ibid.*

[29] D. Boal, Phys. Rev. **C33** (1986) 2206.

[30] T. Csorgo, J. Zimanyi, J. Bondorf and H. Heiselberg, NORDITA preprint (1988).

[31] A.H. Mueller and J. Qiu, Nucl. Phys. **B268** (1986) 427.

[32] J.P. Blaizot and A.H. Mueller, Nucl. Phys. **B289** (1987) 847.